Proceedings World Geothermal Congress 2020+1
Reykjavik, Iceland, April - October 2021

Scaling and Corrosion Control in a High Chloride Geothermal Brine

Keith Lichti[1], Rosalind Julian[1], Kevin Brown[2], Gener Villafuerte[3] and Richard Dambe[3]

[1]Quest Integrity NZL Limited, P O Box 38096, Lower Hutt 5045, New Zealand

[2]GEOKEM, P O Box 30-125, Barrington, Christchurch 8244, New Zealand

[3]Newcrest Mining Limited – Lihir, Lihir Island, New Ireland Province, Papua New Guinea

R.Julian@QuestIntegrity.com; kevin@geokem.co.nz; Gener.Villafuerte@newcrest.com.au

Keywords: Lihir, silica, calcite, scaling, control, pH adjust, corrosion, chloride, alkali

ABSTRACT

The Lihir geothermal wells typically produce two phase fluid with neutral to slightly alkaline brine. The brines are high in dissolved salts. Silica saturation levels can lead to scaling in separation plant, in reinjection wells and in the injection formation. Control of silica scaling in the high chloride waters by acidification to delay polymerisation was considered to present an unacceptably high risk of corrosion of carbon steels used for process piping and steam separation plant as well as reinjection wells. Increasing the pH was seen as a viable alternative solution to increase the silica solubility at selected reinjection temperatures and avoid the risks identified for acid corrosion. A pilot plant designed to give controlled reduction of brine temperature in a small bore heat exchanger was used to test carbon steel corrosion rates under simulated heat exchange and reinjection conditions. The results obtained showed silica could be kept in solution under the selected conditions. However, onset of calcite scaling was observed in the test plant as a result of the well mix used for testing and the test arrangement that appeared to promote flashing. A low and acceptable corrosion rate of carbon steel was measured for the alkaline pH conditions tested, this being potentially due to the favorable pH, or the formation of thin protective silica scales or calcite scaling. Standby corrosion resulting from residual chlorides present after shutdown led to onset of localized corrosion of the order 0.1 mm on the corrosion models used.

1. INTRODUCTION

The Newcrest operated gold mine on Lihir Island generates electricity from a mix of geothermal steam and diesel power plants. Reinjection of geothermal brine provides opportunity to enhance production, and added heat exchange of this brine, provides opportunity for enhanced energy recovery.

A significant constraint on the low temperature energy extraction is the risk of silica scaling, both in heat exchange equipment and in reinjection wells. Use of pH adjustment by acid addition to delay silica polymerisation and allow lower temperature transport and reinjection was risk assessed with respect to heavy metal precipitation and corrosion. A significant risk was identified for the produced brine as follows:

- The produced fluids, at pH 8, showed evidence for absence of corrosion in the present separators and pipelines, this being attributed to thin layers of amorphous silica precipitating.
- The chemistry was considered severe with respect to chloride concentrations (16,000 to 18,000 mg/kg).
- Antimony and other heavy metals were expected to deposit under acid pH adjustment.
- Acidification would have a high risk for corrosion of carbon steel heat exchange (HE) tubes unless the silica scales that formed were still able to block the solution from the steel.
- Under more alkali conditions the corrosion of carbon steel HE tubes was not predicted to become excessive.

The use of alkali pH conditions to increase the solubility of silica in the chloride rich brine would provide ease of operation since:

- Carbon and low alloy steels, compliant with ANSI, NACE MR0175 / ISO 15156 (Part 2) for resistance to Sulfide Stress Corrosion Cracking could be specified in preference to Corrosion Resistant Alloys required for acidic high chloride conditions.
- Under stand-by conditions carbon steels would have lower risk of localized corrosion.
- Lower cost Corrosion Resistant Alloy compliant with ANSI, NACE MR0175 / ISO 15156 (Part 3) for resistance to Sulfide Stress Corrosion could be specified.
- Risk of Chloride Stress Corrosion Cracking for austenitic stainless steels and nickel-base alloys having < 42% Ni would be reduced.
- Alkaline Stress Corrosion Cracking in solutions up to pH 11 was not predicted unless caustic concentration occurred. The risk could be further reduced by thermal stress relief of welded carbon steels.
- Antimony and arsenic sulfides will not deposit.

The benefits of alkali pH adjustment were considered significant and a test programme was initiated to confirm the alkali pH required for silica scale control and to determine the corrosion rate of carbon steel in the alkali treated brines. A purpose built prototype heat exchanger was constructed for this work and is described in detail by Erstich et al, 2012. This paper summarises results for the tests completed with alkali pH adjusted Lihir brines.

2. SILICA SOLUBILITY TRIALS

In the absence of pH adjustment silica polymerisation at low temperature was rapid, as shown for operation of the heat exchanger with no dosing and an exit temperature of 100 °C, see Figure 1a. The room temperature pH of this brine was 8.4. Modelling of this

fluid indicated that at 85 ºC, a pH of 9.4 (measured at 25ºC) was required to completely dissolve all of the silica present. Testing at pH 9.5 and 85 ºC for 180 minutes confirmed the modelling, Figure 1b. Although the temperature stability was less than ideal, recorded temperatures varying from 77ºC to 93ºC, the silica polymerisation shown in Figure 1b indicated that the monomeric silica concentrations were within experimental error, indicating that no silica polymerisation was taking place.

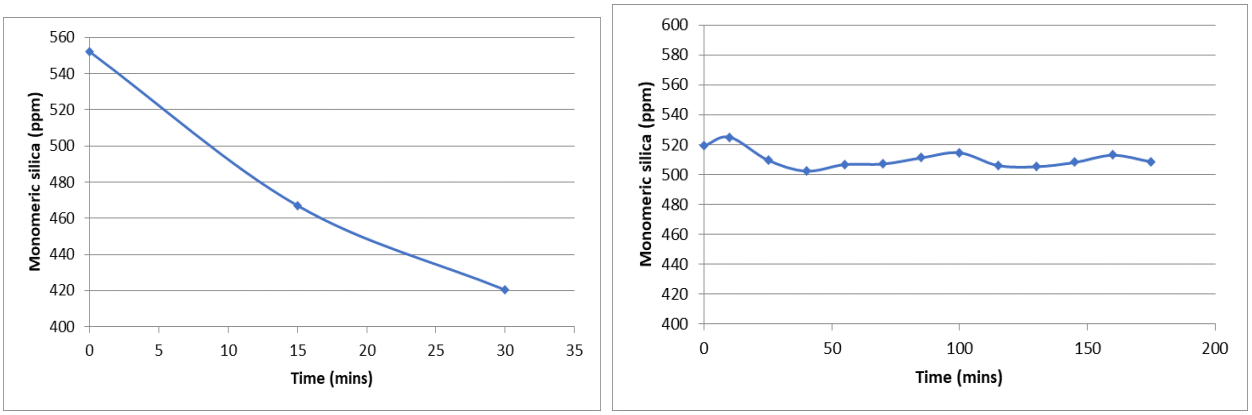

a) Silica polymerisation at 100 ºC at pH 8.4.

b) Silica polymerisation at 85 °C and pH = 9.5.

Figure 1: Silica polymerisation at 100 °C with no adjustment and at 85 °C at alkali pH of 9.5. Graphs show silica concentration in mg/kg vs time in minutes.

These results prompted additional tests at lower pH as summarized in Figure 2. At pH = 9.27 and at pH 8.9 there appeared to be little or no silica polymerisation. The results at these lower pH values indicated an initial decrease in monomeric silica concentration followed by a constant concentration which suggests that there was a small amount of initial silica polymerisation and then equilibrium solubility was reached and no further polymerisation took place. In all of the tests there was some difficulty in controlling the temperature which was the reason for the variations with time seen in Figure 1b and Figure 2.

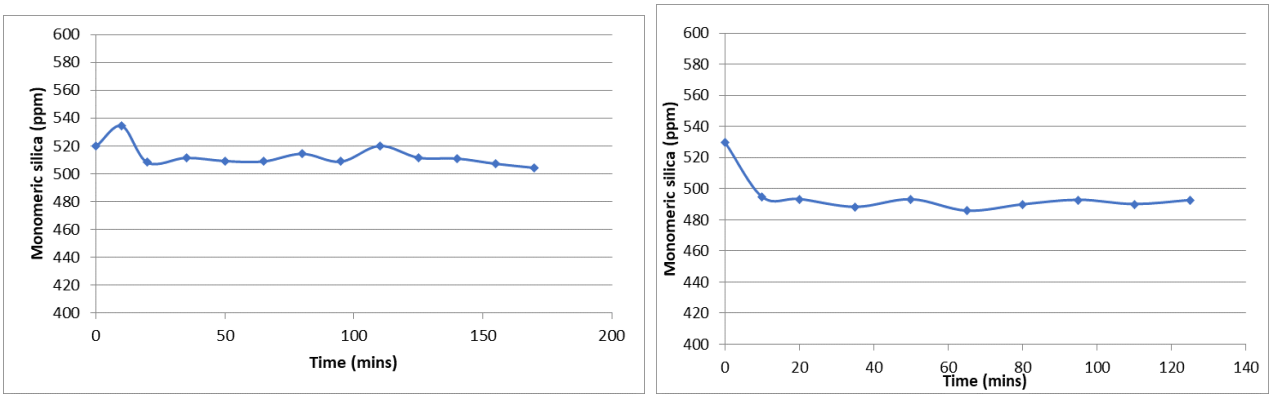

a) Silica polymerisation at 85 ºC and pH 9.27.

b) Silica polymerisation at 85 °C and pH = 8.9.

Figure 2: Silica polymerisation at 85 °C with pH adjustment at alkali pH of 9.27 and 8.9. Graphs show silica concentration in mg/kg vs time in minutes.

3. SHORT TERM ON-LINE CORROSION RATE TEST CONDITIONS

The heat exchanger test rig used 13.8 mm internal diameter tube with two separate streams, one with no pH adjustment (A line) and one with caustic dosing (B line). Corrosion test loop access points were incorporated in the design at the fluid entry and exit points of the heat exchanger tubes. The entry temperature of the brine was of the order 140 °C and the exit temperature was targeted to 110 °C for the corrosion studies. Process water from a nearby water treatment plant was used for cooling of the tubes using purpose built water jackets.

A first series of parallel tests, Tests 1 through 3, as shown in Table 1, were completed for one set of well combinations feeding the plant. A second set of tests with another well combination were then completed, Tests 4 through 6 as shown Table 1. Carbon steel electrical resistance (ER) Corrosometer [TM11] probes were exposed in-line using a T arrangement as shown in Figure 3 to give a

[1] Trade Mark, Coasaco Corroison Monitoring and Chemical Management Systems, USA.

measure of accumulated material loss. Linear Polarisation Resistance (LPR) probes were used to measure instantaneous corrosion rates and the removable electrodes used gave opportunity for a measure of mass gain/loss for the pH condition and exposure time of the tests. A Computational Fluid Dynamic (CFD) model for this small bore pipe design was generated but with the T horizontal whereas the implementation was with a downward exit as illustrated in Figure 3, see Lichti et al (2020). The flow rate used gave linear velocities for the test element in the range 1.4 to 1.8 m/sec and a wall shear stress of the order 20MPa. The ER corrosion monitors used here were previously described by Lichti and Julian (2010).

Table 1: On-Line Corrosion Rate Testing Programme.

Test No	Line	Temperature	pH(25 °C)	Exposure Time
		°C		hours
1	A	Inlet 145, Outlet 112	8.0	5
1	B	Inlet 141, Outlet 111	9.0	5
2	A	Inlet 144, Outlet 111	8.0	5
2	B	Inlet 140, Outlet 111	9.5	5
3	B	Inlet 137, Outlet 102	10.0	3
4	B	Outlet 85	9.5	5
5	B	Outlet 85	9.0	3
6	B	Outlet 85 Outlet 85 Outlet 85	9.0 9.5 10.0	3 then 2 then 2

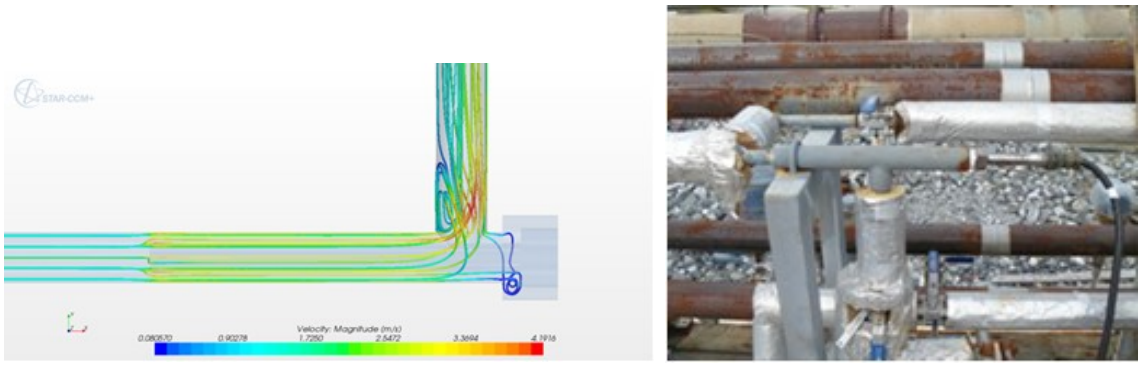

a) CFD Flow Modelling with horizontal exit, 1,000 kg/h b) On-line Implementation with downward pipe exit

Figure 3: Example on-line access point for ER probes in the 13.8 mm heat exchange tubes. Actual flow conditions achieved were 400 to 600 kg/hour with the downward flow velocity controlled by the exit valve for the T.

4. ON-LINE CORROSION RATE TEST RESULTS

The on-line ER corrosion rate measurements indicated low and acceptable corrosion under all conditions tested. Figure 4 illustrates the results for pH10 (25 °C) obtained in Test 3, these being typical for the 6 tests completed. Low accumulated material loss results were indicated with considerable scatter in the readings obtained with the measurement instruments used. The extrapolation method used was outlined by Lichti et al (2010) The primary reason for the observed scatter was the high local temperatures and limitations with the electronics of the monitoring instruments being used. Extrapolation techniques for these short term test results to one year indicated corrosion rates less than 0.15 mm/year. Table 2 provides a summary of the results obtained from ER probes. The corrosion rates were all less than 0.15 mm/year.

On-line LPR corrosion rate measurement results are summarized in Table 3. There was significant difficulty in obtaining reliable LPR results as a consequence of both the local environment temperature and electrode scale formation. This method of corrosion rate measurement requires that the test electrode is freely corroding and readily polarized by an external applied current and that the surface area exposed is unchanging (see Lichti and Wilson, 1980). The potential of the test electrode drifted on polarization and often failed to return to rest potential when the polarization current was removed. Although some error was associated with the results obtained the corrosion rates for tests 1 through 5 were similar to those obtained using the ER probes and were less than 0.11 mm/year at the end of the experiments. The test 6 results were higher at 0.35 mm/year (measured after an attempt at calibration of the heat affected instrument) but interestingly showed little change from pH 9 to pH 10.

The mass loss results obtained on the removable electrodes were not considered representative of the long term corrosion as the exposure times were too short. Pitting corrosion, associated with brown spotting, was observed on the ER probes after extended storage. This was attributed to shutdown/standby corrosion of the exposed monitors that readily occurred despite attempts to remove and dry the samples after exposure and to keep them dry in transport. Table 4 gives a summary of the pitting results for the ER probes. The pit depths were to a common depth 0f 0.1 mm which is typical of shutdown corrosion at a single plant outage (see for example Braithwaite and Lichti (1981))

A significant difference in the scaling rate was observed between tests 1 to 3 vs tests 4 to 6 with the initial tests showing mainly thin films analyzed by Scanning Electron Microscope Energy Dispersive X-Ray Analysis as containing Si and O (presumed as

silica) and the latter tests showing mainly Ca, O and C (verified as calcite, $CaCO_3$, by X-Ray Diffraction). The well mix for the second series of tests included wells that did not have calcite antiscalant added and the pressure drop across the probes inserted into the small bore pipes was taken as contributing to the enhanced calcite scaling as is illustrated in Table 3 for the "in" LPR probe results for the B line scale thickness results for tests 4 through 6 compared to the scale thickness vales for tests 1 through 3.

An interesting additional deposit scale was seen in the earlier tests where small deposits rich in Na, S and O were also observed (identified as thenardite, Na_2SO_4, by X-Ray Diffraction) thought to have precipitated on shutdown by residual brine flashing. No iron based corrosion products were detected by XRD.

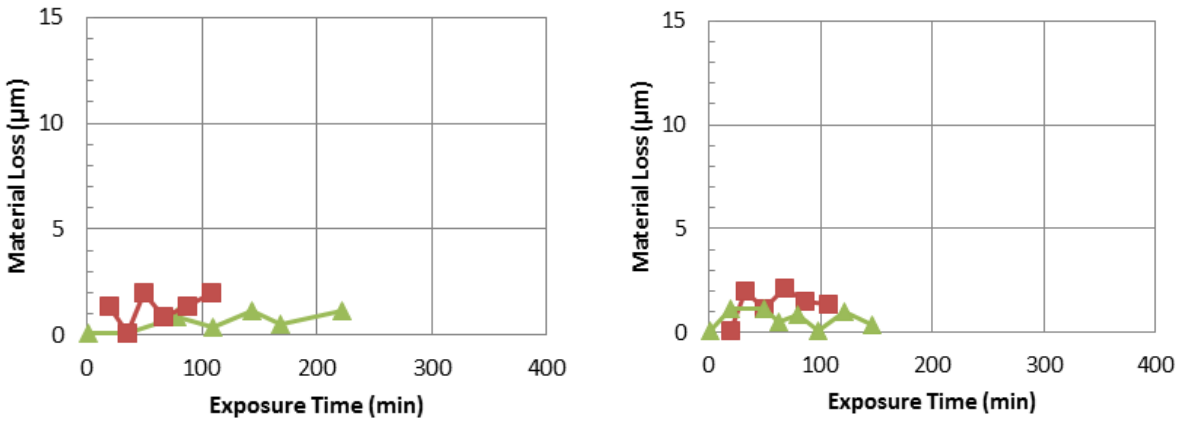

a) Test 3, pH 10, in (left) at 136.6 to 138.6 °C and out (right) at 93.3 to 110.9 °C, ER Probe Material Loss results obtained using two differing meters.

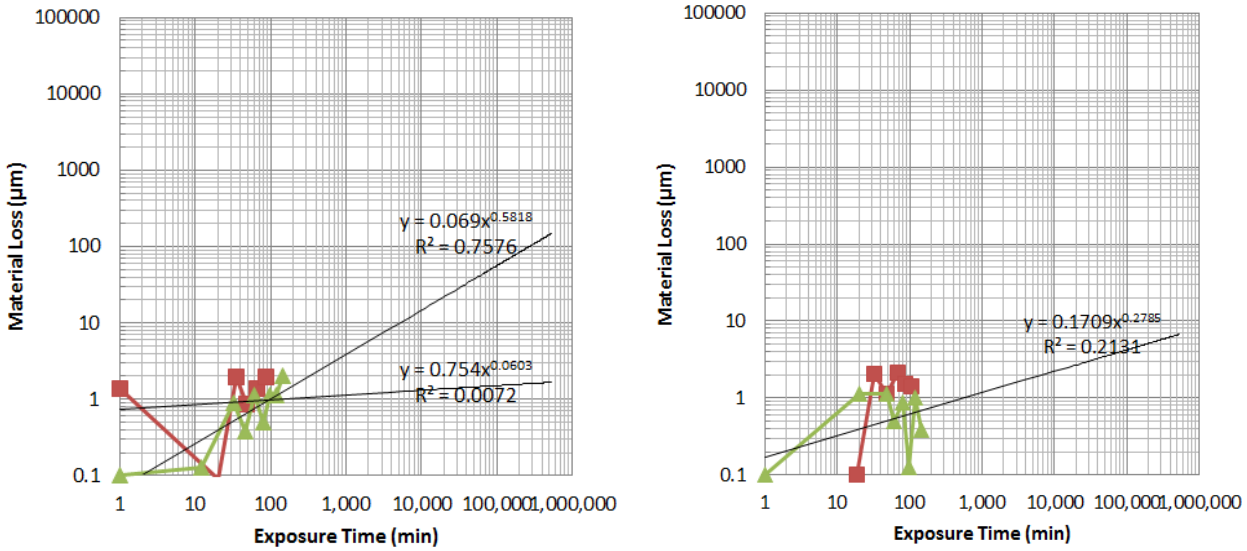

b) Extrapolation technique for results obtained from Test 3 after 3.3 hours to one year following the method of Lichti et al (2010).

Figure 4: Example on-line ER probe results and extrapolation to one year.

Table 2: Summary of ER probe on-line test results extrapolated to one year.

Test No	Location	Condition		Temperature	Flow Rate	Est Pipe Velocity	Est Probe Velocity	Pred CR	Deposition	Appearance
		Target	Actual	Range	ton/hour	From CFD Model - Adj from 1 ton/hour		mm/year	Observed	After Drying
		pH	pH	C		m/sec	m/sec			
Test 1	Ain	8	8	144 to 146	0.6	1.2	1.8	0.01	No	Grey Spots/Swirls
	Aout	8	8	106 to 119	0.6	1.2	1.8	0.1	No	Black Spots/Bright
	Bin	9	8.8	141 to 142	0.49	0.98	1.47	0.1	Local Exit Area	Black Spots
	Bout	9	8.8	107 to 115	0.49	0.98	1.47	0.05	No	Brown spots/Swirls
Test 2	Ain	8	8	143.6 to 144.6	0.6	1.2	1.8	0.03	No	Tan with Grey/Black Swirls
	Aout	8	8	102.3 to 120.8	0.6	1.2	1.8	<0.2	No	Dark pattern/White swirls
	Bin	9.5	9.3	139.1 to 140.6	0.5	1	1.5	Low	Local Exit Area	Light Grey/Dark areas
	Bout	9.5	9.3	105.4 to 118.8	0.5	1	1.5	Low	No	Dark/Dark Grey Pattern
Test 3	Bin	10	10	136.6 to 138.6	0.46	0.92	1.38	0.15	Whole probe	White Deposit
	Bout	10	10	93.3 to 110.9	0.46	0.92	1.38	<0.01	No	Black Film/Spotty Pattern
Test 4	Bin	9.5	9.5	138 to 140	0.55	1.1	1.65	Low	Yes	White Scale/Flaking
	Bout	9.5	9.5	78 to 91	0.55	1.1	1.65	Low	No	Bright/Black Spots
Test 5	Bin	9	9	138 to 140	0.5	1	1.5	Low	Yes	White Scale/Flaking
	Bout	9	9	77 to 93	0.5	1	1.5	Low	No	Dull Grey/Black Areas
Test 6	Bin	9, 9.5, 10		134 to 137	0.4	0.8	1.2	Low	Yes	White Scale/Flaking
	Bout	9, 9.5, 10		70 to 92	0.4	0.8	1.2	Low	No	Dull Grey/Black Areas

Table 3: Summary of carbon steel corrosion rate predictions from exposed LPR probes and observed thickness of scales as calculated from mass gain.

Test	Line	Nominal Values		LPR Start	LPR End	Predicted	Scale
		pH	Temp	CR	CR	CR	Thickness
			C	µm/year	µm/year	mm/year	µm
1	Ain	8.0	140	132	58	0.06	5.5
1	Aout	8.0	110	11	8	0.01	1.6
1	Bin	9.0	140	13	Unstable	0.01	31.9
1	Bout	9.0	110	33	30	0.03	9.7
2	Ain	8.0	140	102	107	0.11	10.7
2	Aout	8.0	110	132	35	0.03	5.7
2	Bin	9.5	140	159	111	0.11	61.7
2	Bout	9.5	110	25	57	0.06	11.6
3	Bin	10.0	140	93	92	0.09	26.3
3	Bout	10.0	100	91	25	0.03	5.4
4	Bin	9.5	140	56	41	0.04	395.7
4	Bout	9.5	85	60	33	0.03	10.7
5	Bin	9.0	140	76	57	0.06	181.6
5	Bout	9.0	85	44	48	0.05	7.5
6	Bin	9.0	140	635	318	0.32	
6	Bout	9.0	85	635	413	0.41	
6	Bin	9.5	140	349	349	0.35	
6	Bout	9.5	85	191	349	0.35	
							End
6	Bin	10.0	140	381	349	0.35	375.0
6	Bout	10.0	85	349	349	0.35	7.7

Table 4: Summary of pitting results attributed to standby corrosion on transport and storage for exposed ER probes.

		Corrosometer Test Element Pit Depths - 5 Deepest Pits Measured						
	Pit Density	Pit 1	Pit 2	Pit 3	Pit 4	Pit 5	Mean	Max
	ASTM G46	µm	µm	µm	µm	µm	µm	µm
Test 1 Ain	A3 to A5	76	88	68	70	87	77.8	88
Test 1 A out	A5	61	61	53	64	90	65.8	90
Test 1 Bin	A5	60	66	68	83	54	66.2	83
Test 1 Bout	A3	144	190	97	63	139	126.6	190
Test 2 Ain	< A2	78	105	85	92	89	89.8	105
Tets 2 Aout	A5	97	120	79	97	86	95.8	120
Test 2 Bin	< A3	99	130	116	99	93	107.4	130
Test 2 Bout	< A3	76	70	110	78	105	87.8	110
Test 3 Bin	A5	70	88	111	95	96	92	111
Test 3 Bout	< A3	86	81	84	97	93	88.2	93
Test 4 Bin	< A3	91	126	84	96	126	104.6	126
Test 4 Bout	< A3	93	78	90	80	92	86.6	93
Test 5 Bin	No Pitting							
Test 5 Bout	< A3	99	83	90	90	89	90.2	99
Test 6 Bin	No Pitting							
Test 6 Bout	< A2	83	73	71	65	80	74.4	83

5. SUMMARY AND CONCLUSIONS

Alkali pH adjustment of high chloride near neutral pH fluids derived from the Lihir geothermal field gave increased silica solubility. Testing of carbon steel at original pH of 8.5 and with alkali addition to give pH values of 9.0, 9.5 and 10.0 gave low and acceptable corrosion rates. The low corrosion was attributed to the favorable pH, the presence of thin silica scales and with some wells that were not calcite antiscalant treated, calcite scaling. The high chloride of the Lihir brine gave a high risk of shutdown / standby corrosion and exposed corrosion monitors exhibited a common pit depth after transport and storage of the order 0.1 mm. This standby corrosion risk is predicted for pipelines and heat exchanger tubes exposed to high chloride alkali pH conditions.

6. ACKNOWLEDGEMENTS

The authors express their thanks to Newcrest staff who assisted in the maintenance and operation of the heat exchanger test plant throughout the field work reported here.

REFERENCES

ASTM G46-94(2018), Standard Guide for Examination and Evaluation of Pitting Corrosion, ASTM International, West Conshohocken, PA, 2018, www.astm.org, (2018).ANSI/NACE MR0175/ISO 15156-2015-SG: Petroleum and natural gas industries— Materials for use in H_2S-containing Environments in oil and gas production (Parts 2 and 3), (2015).

Braithwaite W.R., and Lichti K.A.: Surface Corrosion of Metals in Geothermal Fluids, New Zealand, Geothermal Scaling and Corrosion, ASTM STP 717. L A Casper and T R Pinchback, Eds, American Society for Testing and Metals, 1980, pp 81-112. (1981)

Erstich, E., Mejorada. A., Litchi, K. and Brown, K.: Binary Plant Caustic Dosing Test Rig Development, in Proc NZ Geothermal Workshop, Auckland, New Zealand, (2012).

Lichti, K.A., and Julian, R.H.: Corrosion and Scaling in a High Gas (25wt%) Geothermal Fluid, in Geothermal Condensates, World Geothermal Congress, Bali, Indonesia, April (2010).

Lichti K.A., and Wilson, P.T.: The Determination of Metal Corrosion Rates in Geothermal Condensate using Electrochemical Techniques, in Proceedings of the New Zealand Geothermal Workshop, Auckland, November , pp 37-42. (1980)

Lichti, K., Julian, R., Davies, C., Fletcher, B., Osato, K., Sato, M., Kasai, K., Yanagisawa, Y., and Sakura, K.: CFD Modelling Of Corrosion Test Loops for Geothermal Fluid Applications, WGC, Reykjavik, Iceland, April 26 – May 2, (2020).

Lichti, K.A., White, S.P., Ko, M., Villa, Jr. R.R., Siega, F.L., Olivar, M.M.M., Salonga, N.D., Ogena, M.S., Garcia, S.E., Bunning, B.C., and Sanada, N." Acid Well Utilisation Study: Well MG-9D, Philippines, World Geothermal Congress, Bali, Indonesia, April, (2010).